Vector Rational Interpolation Schemes for Erroneous Motion Field Estimation Applied to MPEG-2 Error Concealment

Sofia Tsekeridou, *Member, IEEE*, Faouzi Alaya Cheikh, Moncef Gabbouj, *Senior Member, IEEE*, and Ioannis Pitas, *Senior Member, IEEE*

***Abstract*—A study on the use of vector rational interpolation for the estimation of erroneously received motion fields of MPEG-2 predictively coded frames is undertaken in this paper, aiming further at error concealment (EC). Various rational interpolation schemes have been investigated, some of which are applied to different interpolation directions. One scheme additionally uses the boundary matching error and another one attempts to locate the direction of minimal/maximal change in the local motion field neighborhood. Another one further adopts bilinear interpolation principles, whereas a last one additionally exploits available coding mode information. The methods present temporal EC methods for predictively coded frames or frames for which motion information pre-exists in the video bitstream. Their main advantages are their capability to adapt their behavior with respect to neighboring motion information, by switching from linear to nonlinear behavior, and their real-time implementation capabilities, enabling them for real-time decoding applications. They are easily embedded in the decoder model to achieve concealment along with decoding and avoid post-processing delays. Their performance proves to be satisfactory for packet error rates up to 2% and for video sequences with different content and motion characteristics and surpass that of other state-of-the-art temporal concealment methods that also attempt to estimate unavailable motion information and perform concealment afterwards.**

***Index Terms*—Error concealment, motion field estimation, MPEG-2 compression, temporal concealment, transmission errors, vector rational interpolation.**

I. Introduction

TRANSMISSION of highly compressed video bitstreams (e.g., MPEG-2 video bitstreams) through physical communication channels is liable to errors, being either packet/cell loss or bit errors (isolated or in bursts). These types of errors are usually referred to as *bitstream errors* and they frequently result in loss of the decoder synchronization, which becomes unable to decode until the next resynchronization codeword in the received bitstream. Since resynchronization points are placed at the header of each slice by an MPEG-2 coder, unless otherwise specified, transmission errors may lead to partial or entire slice information loss (loss of prediction errors, coding modes, motion vectors). Such loss of synchronization leads to observable deterioration of the decoded sequence quality, which, in the case of MPEG-2 coding, is further attributed to the use of VLC and differential coding. Furthermore, due to the use of motion-compensated prediction, temporal error propagation to predictively coded frames inside a group of pictures (GOP), i.e., *propagation errors*, leads to even worse results.

A number of methods have been proposed in the literature to achieve error resilience and thus deal with the above-mentioned problem. A nice overview of such methods is given in [1]. One of the ways to solve this problem is the implementation of error concealment (EC) methods at the decoder side. Such methods exploit the spatial and/or temporal correlations inside and among correctly received neighboring regions/frames [2]–[12]. A subclass of EC methods focuses on the "optimal" estimation of erroneously received motion fields based on available surrounding information. Among the methods belonging in this subclass, one may distinguish:

- the *zero motion EC* (ZM EC), which sets lost motion vectors to zero and, thus, performs temporal replacement;
- the *motion-compensated EC* (MC-AV or MC-VM EC), which calculates the average or vector median of adjacent predictively coded motion vectors;
- the *boundary matching algorithm EC* (BMA EC), which defines a number of motion vector candidates and selects the optimal one that minimizes the boundary matching error [13];
- the *motion vector estimation by boundary optimizing EC* (MVE-BO EC), a fast suboptimal version which firstly evaluates the vector median (a MAP motion estimate) of adjacent predictively coded motion vectors, then defines search regions in reference frames around the block pointed at by the vector median, and finally looks for the optimal motion vector by minimizing the boundary matching error [2];
- the *forward-backward block matching EC* (F-B BM EC), which performs temporal block matching of adjacent blocks in order to estimate their "best match" in the reference frames by *MAD* minimization [10];
- the *decoder motion-vector estimation EC* (DMVE EC), a variant of F-B BM EC which, however, uses smaller

Manuscript received October 3, 2001; revised January 7, 2003. This work was supported by the European RTN Project RTN1–1999-00177 – MOUMIR. The associate editor coordinating the review of this manuscript and approving it for publication was Dr. Heather Hong.

S. Tsekeridou is with the Electrical and Computer Engineering Department, Democritus University of Thrace, 67100 Xanthi, Greece (e-mail: tsekerid@ee.duth.gr).

F. A. Cheikh and M. Gabbouj are with the Institute of Signal Processing, Tampere University of Technology, FIN-33101 Tampere, Finland (e-mail: faouzi@cs.tut.fi; Moncef.Gabbouj@tut.fi).

I. Pitas is with the Department of Informatics, University of Thessaloniki, Thessaloniki 54124, Greece (e-mail: pitas@zeus.csd.auth.gr).

Digital Object Identifier 10.1109/TMM.2004.837266

neighboring regions in the temporal matching process to reduce processing delays [11];
- the *bilinear motion field interpolation EC* (BMFI EC), which estimates one motion vector per pixel instead of block using bilinear interpolation among adjacent motion vectors [12];
- the *combined BMFI EC* (Comb. BMFI EC), an extension of the BMFI EC which, additionally, exploits the outcome of the BMA EC [12].

Motivated by the introduction of vector rational interpolation in [14]–[16] and its remarkable performance in the case of color image interpolation/resampling, a study on its use for the estimation of erroneously received motion fields of predictively coded frames inside an MPEG-2 compressed video bitstream is undertaken in this paper. It is evident that the presented methods may be used alongside any hybrid coder that uses predictive coding. A number of different motion vector rational interpolation schemes are investigated in this paper for EC purposes. Initially, four distinct interpolation schemes are presented differing in which pairs of adjacent motion vectors are used in the vector rational interpolation function, i.e., toward which direction the interpolation takes place. Then, the additional concept of boundary matching error minimization is incorporated in the presented approaches to select the optimal estimation out of the four estimated motion vector candidates. Another scheme attempts to locate the direction of minimum change in the local motion field neighborhood, based on adjacent information, and to perform vector rational interpolation in that direction. Another variant has introduced concepts similar to the ones presented in [12] by including bilinear interpolation principles to the motion vector rational interpolation approach and by introducing a finer interpolation grid in order to further exploit existing spatial correlations. Finally, existing information about the coding modes of adjacent macroblocks (MBs) is exploited and motion vector rational interpolation is employed only among the available inter-coded neighbors. The performance of all presented schemes is compared against that of the motion-compensated temporal ECs mentioned above by judging from the achieved visual quality of the concealed video sequences and by comparing the processing time required for concealment and the accuracy of the restored motion field. Such concealment methods perform satisfactorily in cases of low- to medium-valued packet error rates (PER). For higher PERs, a satisfactory solution is the combination of layered coding with EC methods [7], [17].

The organization of the paper is as follows. In Section II, the mathematical definition and the principles of vector rational interpolation are briefly summarized. In Section III, a variety of motion vector rational interpolation methods are presented for EC of predictively coded frames. Simulation results are reported in Section IV and conclusions are drawn in Section V.

II. Vector Rational Interpolation

Vector rational interpolation has been introduced in [14]–[16] for color image interpolation/resampling applications, where every pixel is represented as a 3-component vector in a color space, in order to exploit the inherent correlations among different color components. The input/output relationship of a vector rational function (**VRF**), according to the definition given in [14], is given by

$$\begin{aligned}\mathbf{VRF} &= \mathbf{RF}[\mathbf{x}_1, \mathbf{x}_2, \ldots, \mathbf{x}_m] = \frac{\mathbf{P}(\mathbf{x}_1, \mathbf{x}_2, \ldots, \mathbf{x}_m)}{Q(\mathbf{x}_1, \mathbf{x}_2, \ldots, \mathbf{x}_m)} \\ &= [rf_1, rf_2, \ldots, rf_l]^T \end{aligned} \tag{1}$$

where $\mathbf{x}_1, \mathbf{x}_2, \ldots, \mathbf{x}_m$ are l-component input vectors to the filter, $\mathbf{P}$ is a vector-valued polynomial, Q a scalar one and rf_i the ith component of the **VRF** output given by

$$rf_i = \left[\frac{P_i(\mathbf{x}_1, \mathbf{x}_2, \ldots, \mathbf{x}_m)}{Q(\mathbf{x}_1, \mathbf{x}_2, \ldots, \mathbf{x}_m)}\right] \tag{2}$$

where

$$\begin{aligned} P_i(\mathbf{x}_1, \mathbf{x}_2, \ldots, \mathbf{x}_m) &= \alpha_0 + \sum_{k=1}^{m} \alpha_k x_k^i \\ &\quad + \sum_{k_1=1}^{m}\sum_{k_2=1}^{m} \alpha_{k_1 k_2} x_{k_1}^i x_{k_2}^i + \cdots \end{aligned} \tag{3}$$

$$Q(\mathbf{x}_1, \mathbf{x}_2, \ldots, \mathbf{x}_m) = b_0 + \sum_{j=1}^{m}\sum_{k=1}^{m} b_{jk} ||\mathbf{x}_j - \mathbf{x}_k||_p. \tag{4}$$

$||.||_p$ denotes the L_p vector norm, $[.]$ denotes integer part, the coefficients $b_0 > 0$, b_{ij} are constant real numbers, whereas the coefficients $\alpha_{i_1, i_2, \ldots, i_n}$ are expressed as a nonlinear function of the input vectors

$$\alpha_{i_1, i_2, \ldots, i_n} = f(\mathbf{x}_1, \mathbf{x}_2, \ldots, \mathbf{x}_m). \tag{5}$$

If $l = 1$, (1) reduces to the scalar rational function input/output relationship.

III. Motion Vector Rational Interpolation EC Schemes

In this section, we investigate the use of properly defined vector rational interpolation functions in the estimation process of erroneously received motion fields of predictively coded video frames. Information loss due to transmission errors in MPEG-2 compressed video data translates to missing motion vectors, coding modes and prediction errors of the respective MBs. If default synchronization is used by the MPEG-2 encoder, i.e., resynchronization points exist at the start of each slice, which is an entire row of MBs, only correctly received top and bottom adjacent block data is available for the estimation of the lost one. In subsequent subsections, a number of different motion vector rational interpolation approaches are introduced. The aim of all presented schemes is to estimate the lost motion vector(s) in the best possible way by using information from available adjacent motion vectors. The neighborhood considered in all interpolation schemes is shown in Fig. 1. After the lost motion vector has been estimated in the way presented in subsequent subsections, concealment of predictively coded frames is performed by copying the displaced block of the previously decoded frame with respect to the estimated motion vector to the current lost one. In the case of B-frames, where two motion fields are available (forward and backward), lost motion vector estimation is accomplished in both fields and

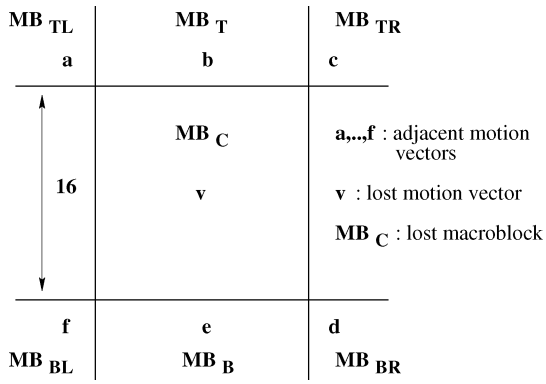

Fig. 1. Neighborhood employed in the motion field interpolation approaches.

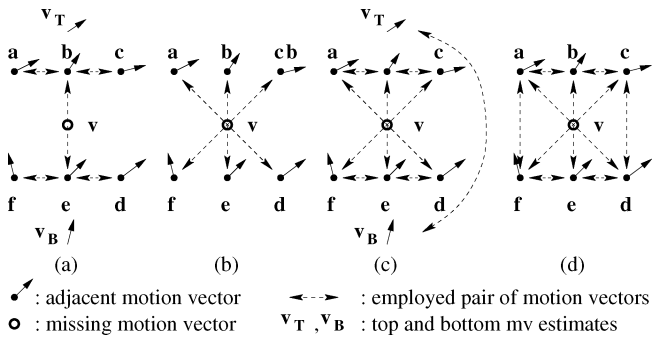

Fig. 2. MVRI schemes: (a) 2-stage 1-D case; (b) 2-D case; (c) 2-stage combined 1-D and 2-D case; and (d) 2-D case considering all directions.

the estimate that leads to the minimum boundary matching error (refer below for definition) is selected for concealment. Intra-coded frames are concealed by the F-B BM EC [10]. Motion vector rational interpolation can also be employed for recovering lost concealment motion vectors of I-frames when such are generated and transmitted.

A. Introduction of Four Distinct Approaches

In a first approach, *four different interpolation schemes* have been considered [18], differing only in the neighboring pairs of available motion vectors used, that is, in which direction the interpolation is applied, as is shown in Fig. 2. They are described in the sequel:

2-Stage 1 – D Case [Fig. 2(a)]:

Horizontal Interpolation: Initially, estimates $(\mathbf{v}_T, \mathbf{v}_B)$ of the top and bottom adjacent motion information are obtained by applying the 1-D vector rational interpolation function

$$\mathbf{v}_T = \frac{\sum_{(\mathbf{u},\mathbf{w})\in S_1} w_{\mathbf{uw}}(\mathbf{u}+\frac{1}{2}\mathbf{w})}{\frac{3}{2}\sum_{(\mathbf{u},\mathbf{w})\in S_1} w_{\mathbf{uw}}} \tag{6}$$

$$\mathbf{v}_B = \frac{\sum_{(\mathbf{u},\mathbf{w})\in S_2} w_{\mathbf{uw}}(\mathbf{u}+\frac{1}{2}\mathbf{w})}{\frac{3}{2}\sum_{(\mathbf{u},\mathbf{w})\in S_2} w_{\mathbf{uw}}} \tag{7}$$

where $S_1 = \{(\mathbf{a},\mathbf{b}),(\mathbf{c},\mathbf{b})\}$, $S_2 = \{(\mathbf{d},\mathbf{e}),(\mathbf{f},\mathbf{e})\}$ and coefficients $w_{\mathbf{uw}}$, $\mathbf{u},\mathbf{w} \in \{\mathbf{a},\mathbf{b},\mathbf{c},\mathbf{d},\mathbf{e},\mathbf{f}\}$, $\mathbf{u} \neq \mathbf{w}$, are defined by

$$w_{\mathbf{uw}} = \frac{1}{1+k\|\mathbf{u}-\mathbf{w}\|}. \tag{8}$$

In (8), $\|.\|$ denotes the L_2 vector norm and k is a positive constant that controls the degree of nonlinearity of the rational filter.

Vertical Interpolation of Horizontal Estimates: The lost motion vector is finally estimated by averaging the horizontal estimates $\mathbf{v}_T$ and $\mathbf{v}_B$

$$\mathbf{v} = \frac{\mathbf{v}_T + \mathbf{v}_B}{2}. \tag{9}$$

2-D Case [Fig. 2(b)]: This interpolation scheme estimates the lost motion vector $\mathbf{v}$ by employing the expression

$$\mathbf{v} = \frac{\sum_{(\mathbf{u},\mathbf{w})\in S} w_{\mathbf{uw}}(\mathbf{u}+\mathbf{w})}{2\sum_{(\mathbf{u},\mathbf{w})\in S} w_{\mathbf{uw}}} \tag{10}$$

where $S = \{(\mathbf{a},\mathbf{d}),(\mathbf{b},\mathbf{e}),(\mathbf{c},\mathbf{f})\}$ and $w_{\mathbf{uw}}$ is given by (8).

2-Stage Combined 1-D and 2-D Case [Fig. 2(c)]:

Horizontal Interpolation: It is performed in the same way as in the 1-D case.

Combined Interpolation: The horizontal estimates of the previous stage are used as input motion vectors along with the input motion vectors of the 2-D case to estimate the lost motion vector

$$\mathbf{v} = \frac{\sum_{(\mathbf{u},\mathbf{w})\in S} w_{\mathbf{uw}}(\mathbf{u}+\mathbf{w})}{2\sum_{(\mathbf{u},\mathbf{w})\in S} w_{\mathbf{uw}}} \tag{11}$$

where $S = \{(\mathbf{a},\mathbf{d}),(\mathbf{b},\mathbf{e}),(\mathbf{c},\mathbf{f}),(\mathbf{v}_T,\mathbf{v}_B)\}$ and $w_{\mathbf{uw}}$ is again given by (8).

2-D Case of All Directions [Fig. 2(d)]: This interpolation scheme is an extension of the 2-D case, in the sense that almost all directions between neighbors are considered in the final estimation

$$\mathbf{v} = \frac{\sum_{(\mathbf{u},\mathbf{w})\in S} w_{\mathbf{uw}}(\mathbf{u}+\mathbf{w})}{2\sum_{(\mathbf{u},\mathbf{w})\in S} w_{\mathbf{uw}}} \tag{12}$$

where now

$$S = \{(\mathbf{a},\mathbf{d}),(\mathbf{b},\mathbf{e}),(\mathbf{c},\mathbf{f}),(\mathbf{a},\mathbf{b}),(\mathbf{b},\mathbf{c}),(\mathbf{f},\mathbf{e}),(\mathbf{e},\mathbf{d}),(\mathbf{a},\mathbf{f}),(\mathbf{c},\mathbf{d})\}.$$

All interpolation schemes attempt to estimate lost motion information in such a way that motion field smoothness is attained in smooth motion areas, while at the same time irregular motion of adjacent blocks does not result in high estimation errors. Intra-coded neighbors are simply considered here as having zero valued motion vectors. No coding mode information of adjacent blocks is exploited at this point. In smooth motion areas, where Euclidean distances between adjacent vectors are small, the weights $w_{\mathbf{uw}}$ are close to 1.0, thus leading to an averaging interpolator. When Euclidean distances increase, the respective weights decrease, thus limiting the contribution of the respective candidate neighboring pair in the final motion vector estimate.

B. Boundary Matching Error Minimization

In a second approach, *the boundary matching criterion* has been employed in order to locate that interpolation scheme out of the four above-mentioned ones that estimates the "optimal"

motion vector with respect to the minimum boundary matching error [13] and thus leads to the best possible concealment, as shown in (13), at the bottom of the page, where $N \times N$ denotes the block size, (x_0, y_0) the spatial coordinates of the top-left pixel of the lost block, f_r the reference frame (forward or backward), f_c the current frame, and $\mathbf{v}_i = (dx_i, dy_i)$, $i = 1, \ldots, 4$ the estimated motion vector by each one of the four interpolation schemes.

C. Interpolation in the Direction of Minimum Change

In a third approach, interpolation has been attempted in the direction of minimal change while preserving the transition in the direction of maximal change inside a predefined motion field neighborhood, in an inverse manner than that of method [19], which aims at image enhancement using rational control functions of the rate of change of the local image content. In order to find the rate and direction of change (maximal or minimal) inside a predefined motion vector neighborhood, an approach similar to the one proposed in [20] has been adopted. Let $\mathbf{MF}(x, y)$, $I\!R^2 \rightarrow I\!R^2$ be a two-valued two-dimensional function denoting the estimated motion field of a frame, i.e., $\mathbf{MF}(x, y) = [Dx(x, y) \;\; Dy(x, y)]^T$, where Dx and Dy, $I\!R^2 \rightarrow I\!R$, represent the functions of the horizontal and vertical displacements composing the motion vectors at points (x, y). When the Euclidean distance of two points (x_1, y_1) and (x_2, y_2) tends to zero, the difference of the values of $\mathbf{MF}(x, y)$ at those points, $\Delta\mathbf{MF} = \mathbf{MF}(x_1, y_1) - \mathbf{MF}(x_2, y_2)$, becomes the arc element

$$d\mathbf{MF} = \frac{\partial \mathbf{MF}}{\partial x} dx + \frac{\partial \mathbf{MF}}{\partial y} dy. \tag{14}$$

Its squared norm, known as the first fundamental form, is given by

$$d\mathbf{MF}^2 = \begin{bmatrix} dx \\ dy \end{bmatrix}^T \begin{bmatrix} g_{xx} & g_{xy} \\ g_{yx} & g_{yy} \end{bmatrix} \begin{bmatrix} dx \\ dy \end{bmatrix} \tag{15}$$

where $(g_{xy} = g_{yx})$

$$\begin{aligned} g_{xx} &= \frac{\partial \mathbf{MF}}{\partial x} \cdot \frac{\partial \mathbf{MF}}{\partial x} = \left(\frac{\partial Dx}{\partial x}\right)^2 + \left(\frac{\partial Dy}{\partial x}\right)^2 \\ g_{yy} &= \frac{\partial \mathbf{MF}}{\partial y} \cdot \frac{\partial \mathbf{MF}}{\partial y} = \left(\frac{\partial Dx}{\partial y}\right)^2 + \left(\frac{\partial Dy}{\partial y}\right)^2 \\ g_{xy} &= \frac{\partial \mathbf{MF}}{\partial x} \cdot \frac{\partial \mathbf{MF}}{\partial y} = \left(\frac{\partial Dx}{\partial x}\right)\left(\frac{\partial Dx}{\partial y}\right) + \left(\frac{\partial Dy}{\partial x}\right)\left(\frac{\partial Dy}{\partial y}\right). \end{aligned} \tag{16}$$

According to [20], $d\mathbf{MF}^2$ is a measure of the rate of motion field change in a prespecified direction. The extrema of (15) are obtained in the direction of the eigenvectors of the matrix $\begin{bmatrix} g_{xx} & g_{xy} \\ g_{yx} & g_{yy} \end{bmatrix}$ and the values attained there are the corresponding eigenvalues. Thus, the eigenvectors provide the direction of maximal/minimal change at a given point (θ_+ and θ_-, respectively), whereas the eigenvalues present the maximal/minimal rate of change (λ_+ and λ_-, respectively). The latter, as reported in [20], are estimated by

$$\lambda_\pm = \frac{g_{xx} + g_{yy} \pm \sqrt{(g_{xx} - g_{yy})^2 + 4g_{xy}^2}}{2}. \tag{17}$$

For the calculation of the maximal/minimal rates of change, (17) implies the prior estimation of the local gradients within the expressions of g_{ij}, where $i, j \in x, y$. For such purpose, directional operators (referred to as convolution kernels as well) are defined for each one of six preselected directions within the local motion vector neighborhood: horizontal, vertical, diagonals 45°, 135°, 30°, and 120°, in a manner similar to the one presented in [21], which targets edge detection in color images. Such preselection is deemed necessary since no *a priori* knowledge exists on which direction the local motion field attains the best smoothness properties. For each direction type, due to the vector-valued case, there is more than one rate of change since the minimal rate of change is not 0 [20]. The selection of the "edge-sensing" masks was done bearing in mind the particulars of the lost motion information problem (e.g., missing horizontal neighboring motion vectors). The masks are shown in Table I. The local motion field neighborhood employed for gradient estimation (where the directional operators are applied) is of size 3×3. The goal is to locate that direction toward which the local motion field neighborhood presents the best smoothness properties. Thus, for every gradient direction type, a minimum and a maximum rate of change, $\lambda_{+_{(i)}}$ and $\lambda_{-_{(i)}}$, $i = I, \ldots, VI$, are estimated by (17), based on the already undertaken approaches of [20], [21] for vector-valued cases. For single-valued cases, the minimum rate of change is 0 and only the maximum rate of change is applicable. The differences $\lambda_{+_{(i)}} - \lambda_{-_{(i)}}$ present an appropriate criterion for detecting transitions in the local motion field, as already stated in [20], since a large difference value means that an irregular motion region exists in this position (the change in motion is significant toward every direction), while a small value means that we are in a smooth motion region (the change in motion is similar toward all directions). Our aim is to locate such smoothness properties, if existent within the local neighborhood, and perform interpolation toward that direction (the respective rational weight will be of large value in this case, as it will be later shown). For such purpose, such differences have been chosen to control the estimation of the rational weights in the motion vector rational interpolation approach. Specifically, candidate motion vector estimates are defined for every direction type as the average of those neighboring motion vectors employed by the respective mask (nonzero elements).

$$\mathbf{v}_{\text{opt}} = \arg \min_{i=1,\ldots,4} \sum_{x=x_0}^{x_0+N-1} (f_r(x + dx_i, y_0 + dy_i) - f_c(x, y_0 - 1))^2 + (f_r(x + dx_i, y_0 + N - 1 + dy_i) - f_c(x, y_0 + N))^2 \tag{13}$$

TABLE I
DIRECTIONAL OPERATORS USED TO ESTIMATE GRADIENT VALUES IN DIFFERENT DIRECTIONS

Direction Type	Mask for $\frac{\partial}{\partial x}$	Mask for $\frac{\partial}{\partial y}$
I (horizontal)	$\begin{bmatrix} 1 & -2 & 1 \\ 0 & 0 & 0 \\ 1 & -2 & 1 \end{bmatrix}$	$\begin{bmatrix} 1 & 1 & 1 \\ 0 & 0 & 0 \\ -1 & -1 & -1 \end{bmatrix}$
II (vertical)	none	$\begin{bmatrix} 0 & 1 & 0 \\ 0 & 0 & 0 \\ 0 & -1 & 0 \end{bmatrix}$
III (diagonal, 135^o)	$\begin{bmatrix} 1 & 0 & 0 \\ 0 & 0 & 0 \\ 0 & 0 & -1 \end{bmatrix}$	$\begin{bmatrix} 1 & 0 & 0 \\ 0 & 0 & 0 \\ 0 & 0 & -1 \end{bmatrix}$
IV (diagonal, 45^o)	$\begin{bmatrix} 0 & 0 & 1 \\ 0 & 0 & 0 \\ -1 & 0 & 0 \end{bmatrix}$	$\begin{bmatrix} 0 & 0 & 1 \\ 0 & 0 & 0 \\ -1 & 0 & 0 \end{bmatrix}$
V (diagonal, 120^o)	$\begin{bmatrix} -1 & 1 & 0 \\ 0 & 0 & 0 \\ 0 & 1 & -1 \end{bmatrix}$	$\begin{bmatrix} 1 & 1 & 0 \\ 0 & 0 & 0 \\ 0 & -1 & -1 \end{bmatrix}$
VI (diagonal, 30^o)	$\begin{bmatrix} 0 & 1 & -1 \\ 0 & 0 & 0 \\ -1 & 1 & 0 \end{bmatrix}$	$\begin{bmatrix} 0 & 1 & 1 \\ 0 & 0 & 0 \\ -1 & -1 & 0 \end{bmatrix}$

For example, for type II, the candidate motion vector estimate $\mathbf{v}_{(II)}$ is given by $\mathbf{v}_{(II)} = (\mathbf{b} + \mathbf{e})/2$. In the case of motion uniformity among neighbors, their average presents a good estimate for the lost motion vector. The motion vector estimate in this case is calculated by

$$\mathbf{v} = \frac{\sum_{i=I}^{VI} w_{(i)} \mathbf{v}_{(i)}}{\sum_{i=I}^{VI} w_{(i)}} \tag{18}$$

where the rational weights $w_{(i)}$ are estimated by

$$w_{(i)} = \frac{1}{1 + k(\lambda_{+_{(i)}} - \lambda_{-_{(i)}})}. \tag{19}$$

D. Incorporation of Bilinear Interpolation Principles

Motivated by the approach of [12], the MVRI EC has been extended to include bilinear interpolation principles in order to further exploit spatial correlations. The neighborhood employed in the motion vector rational-bilinear interpolation approach is shown in Fig. 3. The only difference with the neighborhood of Fig. 1 is that a finer interpolation grid is defined according to which one motion vector per 4×4 block inside the lost 16×16 MPEG-2 MB is estimated. Thus, 16 motion vectors $\mathbf{v}_{ij}$, instead of 1, are derived per lost MB. Consequently, the final motion estimate $\mathbf{v}$ is a 4×4 matrix $\mathbf{v} = [\mathbf{v}_{ij}]$, $i, j = 1, \ldots, 4$. The estimation scheme, a combination of vector rational and bilinear interpolation, involves the computation of each $\mathbf{v}_{ij}$

$$\mathbf{v}_{ij} = \frac{\sum_{(\mathbf{u},\mathbf{w}) \in S} w_{\mathbf{uw}} (w_{ij\mathbf{u}} \mathbf{u} + w_{ij\mathbf{w}} \mathbf{w})}{\sum_{(\mathbf{u},\mathbf{w}) \in S} w_{\mathbf{uw}} (w_{ij\mathbf{u}} + w_{ij\mathbf{w}})} \tag{20}$$

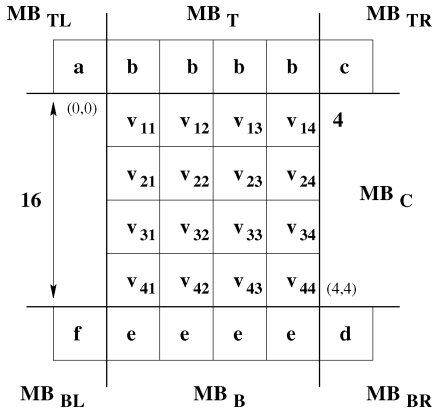

Fig. 3. Graphical presentation of the motion field estimation basis in the MVRI-BMFI method.

where $S = \{(\mathbf{a}, \mathbf{d}), (\mathbf{b}, \mathbf{e}), (\mathbf{c}, \mathbf{f})\}$. Equation (20) is an extension of the $2d$ vector rational interpolation case, presented previously. $w_{\mathbf{uw}}$ are the rational interpolation weights evaluated by (8), which are calculated only once per lost MB, since they are independent of spatial locations. $w_{ij\mathbf{u}}$ represent weights based on spatial locations. For each $\mathbf{v}_{ij}$, a 2×3 matrix $W_{ij} = [w_{ij\mathbf{u}}]$, $\mathbf{u} \in \{\mathbf{a}, \ldots, \mathbf{f}\}$, is defined that contains the spatial location weights. The structure of W_{ij} is proportional to the spatial localization of $\mathbf{v}_{ij}$ with respect to the motion vector neighborhood in Fig. 3. Obviously, 16 such matrices, one per $\mathbf{v}_{ij}$, have to be calculated. They are defined as spatial location look-up tables, because they need to be estimated only once, due to the identical spatial structure of each $\mathbf{v}_{ij}$ inside the motion vector neighborhood for dinstinct lost MBs. This results in computational savings. The spatial weight calculation is done in an identical manner as in bilinear interpolation. Distances from the estimated motion vector to its neighbor estimator are measured in the motion vector coordinate system (see Fig. 3). These are converted to integers for faster computations and less memory requirements. To help the reader understand the estimation process of W_{ij}, we present an example of how W_{24} is estimated, as follows:

$$W'_{24} = \begin{bmatrix} \frac{1}{5} \cdot \frac{3}{5} & \frac{3}{5} & \frac{4}{5} \cdot \frac{3}{5} \\ \frac{1}{5} \cdot \frac{2}{5} & \frac{2}{5} & \frac{4}{5} \cdot \frac{2}{5} \end{bmatrix} \Rightarrow W'_{24} = \frac{1}{25} \begin{bmatrix} 3 & 15 & 12 \\ 2 & 10 & 4 \end{bmatrix} = \frac{1}{25} W_{24}. \tag{21}$$

When an array term is derived from the multiplication of two individual terms, the first one corresponds to the horizontal spatial distance from the existing neighboring motion vector subtracted from 1 and the second one to the vertical such distance subtracted from 1.

This interpolation scheme attempts to estimate lost motion information in such a way that motion smoothness is attained in smooth motion areas (linear operation performs best in such a case), whereas irregular motion of adjacent blocks does not result in high estimation errors (spatial correlations perform well in such cases). Thus, the method attains good motion field characteristics: motion smoothness and motion discontinuity, as long as adjacent motion data is sufficient for correct estimation. Again, intra-coded neighbors are simply considered as having zero valued motion vectors and no coding mode information of adjacent blocks is actually exploited in the estimation process.

TABLE II
CORRESPONDENCE OF ABBREVIATIONS AND INTRODUCED CONCEALMENT METHODS. MVRI ALWAYS STANDS FOR MOTION VECTOR RATIONAL INTERPOLATION AND EC FOR ERROR CONCEALMENT

Abbreviation	Explanation
MVRI-1 – D EC	2-stage 1 – D MVRI
MVRI-2 – D EC	2 – D MVRI
MVRI-Combined EC	2-stage Combined 1 – D and 2 – D MVRI
MVRI-2 – D-All EC	2 – D of all Directions MVRI
MVRI-BM EC	MVRI with boundary matching error minimization
MVRI-RoC EC	MVRI that interpolates in the direction of minimum change
MVRI-BMFI EC	MVRI with bilinear interpolation principles
MVRI-CodM EC	MVRI exploiting available coding mode information

E. Exploitation of Available Coding Mode Information

This scheme additionally exploits available neighboring coding mode information in order to consider solely the inter-coded neighbors in the motion vector rational interpolation approach. Thus, estimation errors due to the intra-coding of neighboring blocks are avoided. The final estimate is evaluated by

$$\mathbf{v} = \frac{\sum\limits_{\mathbf{u},\mathbf{w}\in\{\mathbf{a},\mathbf{b},\mathbf{c},\mathbf{d},\mathbf{e},\mathbf{f}\},\mathbf{u}\neq\mathbf{w}} w_{\mathbf{uw}}(\mathbf{u}+\mathbf{w})}{2\sum\limits_{\mathbf{u},\mathbf{w}\in\{\mathbf{a},\mathbf{b},\mathbf{c},\mathbf{d},\mathbf{e},\mathbf{f}\},\mathbf{u}\neq\mathbf{w}} w_{\mathbf{uw}}} \tag{22}$$

additionally constraining $\mathbf{u}$, $\mathbf{w}$ to be the motion vectors of inter-coded neighbors. After the latter have been singled out based on coding mode information, all possible pairs $(\mathbf{u},\mathbf{w})$ are constructed and employed in (22). The additional use of coding mode information proves to enhance the estimation accuracy.

IV. SIMULATION RESULTS

In order to evaluate the performance of the motion vector rational interpolation methods for EC, three different CCIR 601 sequences at 4:2:0 chroma sampling format have been used, namely the Flower Garden (125 frames), the Mobile & Calendar (40 frames), and the Football (50 frames) sequences. These sequences differ in the type of observed motion, as well as content. The first one is characterized by large uniform global motion (moving camera), the second one by medium-valued nonuniform motion (three objects moving differently), while the last one is characterized by highly irregular motion in many directions. They have been coded at 5 Mbps at 25 fps (PAL) using slice sizes equal to an entire row of MBs and setting the number of frames in a group of pictures (GOP) equal to 12 and the number of frames between successive I- and P-frames or P- and P-frames equal to 3. Layered coding is not employed and motion compensation is performed on a MB basis during encoding (one motion vector per 16×16 block for the luminance component). MPEG-2 transport packets are considered, which are 188 bytes long composed by 4 bytes of header information and 184 bytes of payload. A PER value of 2% has been considered. Errors may result from either isolated bit errors or packet loss. The error locations are assumed known and it is assumed that, once an error is detected, all packets are discarded until the decoder is able to resynchronize. In order to help the reader quickly understand the abbreviations used in the sequel for the methods introduced in this paper, Table II is presented.

TABLE III
AVERAGE PSNR VALUES MEASURED ON THE THREE TEST SEQUENCES (Y COMPONENT) AFTER THEIR CONCEALMENT BY THE METHODS UNDER STUDY FOR A PER VALUE EQUAL TO 2%

EC Method	Flower	Mobile	Football
Error Free	29.75	35.50	32.40
ZM EC	24.10	31.12	26.96
MC-AV EC	26.48	33.13	27.88
MC-VM EC	26.65	33.59	27.92
BMA EC	26.33	33.61	28.10
MVE-BO EC	25.87	32.63	28.14
F-B BM EC	**27.74**	33.85	**28.40**
BMFI EC	26.06	32.90	27.63
Comb BMFI EC	26.49	33.57	28.22
MVRI-1 – D EC	27.22	33.55	28.06
MVRI-2 – D EC	27.31	33.85	28.02
MVRI-Combined EC	27.28	33.82	28.02
MVRI-2 – D-All EC	27.24	33.79	28.01
MVRI-BM EC	27.26	**33.89**	28.12
MVRI-RoC EC	27.29	33.84	28.03
MVRI-BMFI EC	27.32	33.84	28.03
MVRI-CodM EC	**27.72**	**34.00**	**28.41**
Erroneous	13.88	20.14	17.52

Objective performance evaluation of the presented concealment method is based on average PSNR values, whereas subjective evaluation is achieved by observing the visual quality of the concealed sequence. In order to assess the performance of the various motion field estimation processes, the *Motion Field Estimation Error* [$\mathrm{MFE}(t)$] is used

$$\mathrm{MFE}(t) = \frac{1}{b_x \times b_y} \times \sum_{x=1}^{b_x} \sum_{y=1, CM(x,y)\in\{F,B,D\}}^{b_y} \|\mathbf{MF}_{\mathrm{est}}(x,y;t) - \mathbf{MF}_{\mathrm{or}}(x,y;t)\|. \tag{23}$$

In (23), $b_x \times b_y$ represents the total number of block motion vectors in a frame. $CM(x,y)$ represents the original coding mode of the considered MB, which should actually indicate to an inter-coded MB, i.e., forward predicted (F), backward predicted (B), or bi-directionally predicted (D) (original motion information available in this case). $\mathbf{MF}_{or}(x,y;t)$ is the original motion field of the current frame t, whereas $\mathbf{MF}_{est}(x,y;t)$ is the estimated one. Finally, since fast concealment is a requirement for real-time decoding capabilities, the execution time for each of the concealment methods under study is measured.

Table III illustrates the average PSNR values for the luminance component evaluated on the concealed test sequences by

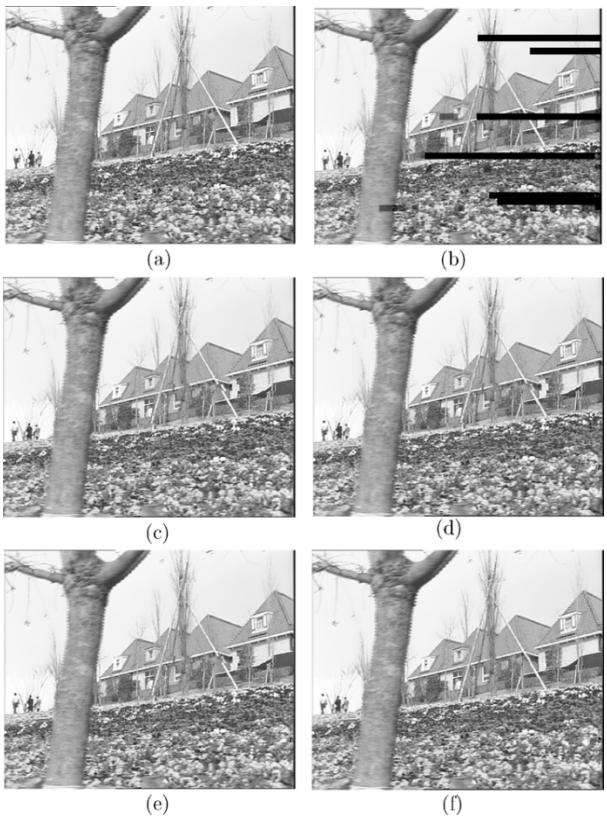

Fig. 4. Frame 25 of the Flower Garden sequence: (a) without errors, (b) with errors, $\mathrm{PER} = 2\%$, concealed by: (c) MC-VM EC, (d) BMA EC, (e) combined BMFI EC, and (f) MVRI-CodM EC.

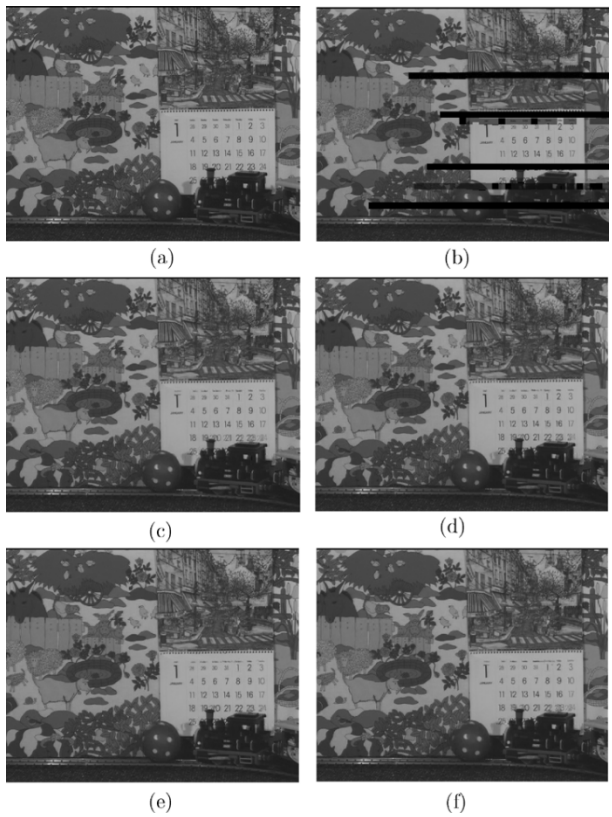

Fig. 5. Frame 26 of the Mobile & Calendar sequence: (a) without errors, (b) with errors, $\mathrm{PER} = 2\%$, concealed by: (c) MC-VM EC, (d) BMA EC, (e) combined BMFI EC, and (f) MVRI-CodM EC.

using all the motion field estimation EC methods under study. It can be seen that, in almost all cases, the motion vector rational interpolation EC schemes as well as the F-B BM EC method attain the best result. The one that distinguishes itself, with respect to PSNR values, among the motion vector rational interpolation approaches is the MVRI-CodM EC method. Its performance is attributed to the fact that this method additionally exploits available neighboring coding mode information, which proves not to be redundant but rather of significance. Their rather satisfactory performance, compared with that of the other motion estimation EC methods under study, can be further established by observing the achieved visual quality of the concealed test sequences. In Figs. 4–6, certain frames of the concealed test sequences Flower Garden, Mobile & Calendar, and Football, respectively, are shown. The methods used for concealment are the MC-VM EC, the BMA EC, the Combined BMFI EC and the MVRI-CodM EC, which lead to the best results with respect to PSNR values shown in Table III. The conclusion is that the motion vector rational interpolation EC schemes lead to satisfactory concealment for cases of medium PER values and achieve smooth concealment, edge and line reconstruction, even in strong motion or irregular motion areas, provided that the neighboring motion information is adequate for the estimation of the lost data. In regions of strong or irregular motion, many of the other state-of-the-art temporal EC methods lead to observable frame content shifts.

Table IV illustrates the temporal *MFE* average values evaluated on the estimated motion fields of predictively coded frames and only for the predictively coded MBs. It is easily observed

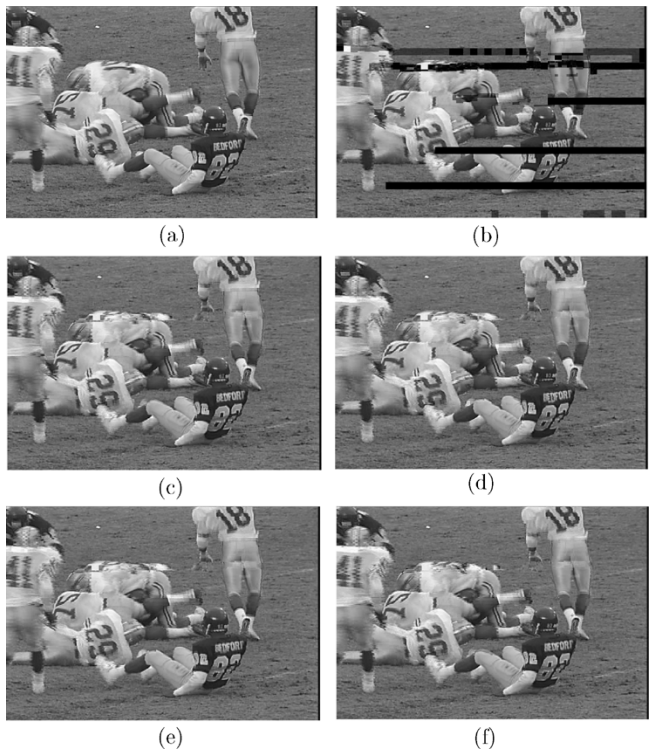

Fig. 6. Frame 25 of the Football sequence: (a) without errors, (b) with errors, $\mathrm{PER} = 2\%$, concealed by: (c) MC-VM EC, (d) BMA EC, (e) combined BMFI EC, and (f) MVRI-CodM EC.

that the MVRI EC methods, especially the one exploiting available coding mode information, lead to small error values, a fact

TABLE IV
AVERAGE MFE VALUES MEASURED ON THE ESTIMATED MOTION FIELDS OF THE PREDICTIVELY CODED FRAMES OF THE THREE TEST SEQUENCES

EC Method	Flower	Mobile	Football
ZM EC	8.87	2.73	8.51
MC-AV EC	3.48	2.27	6.82
MC-VM EC	3.36	2.20	6.67
BMA EC	3.56	2.32	6.32
MVE-BO EC	3.92	2.56	6.27
BMFI EC	3.61	2.37	6.99
MVRI-1 – D EC	2.89	1.95	6.12
MVRI-2 – D EC	2.88	1.96	6.09
MVRI-Combined EC	2.91	1.94	6.11
MVRI-2 – D-All EC	2.92	1.97	6.13
MVRI-RoC EC	**2.86**	1.88	**6.00**
MVRI-BMFI EC	2.87	**1.86**	6.02
MVRI-CodM EC	**2.67**	**1.67**	**5.97**
Erroneous	8.87	2.73	8.51

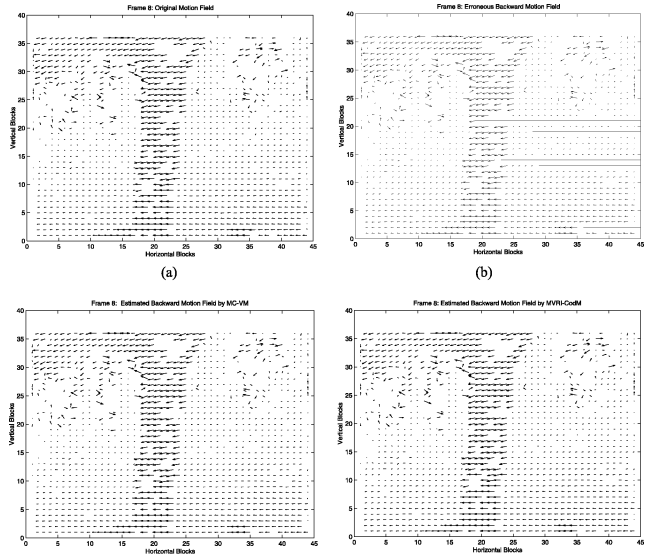

Fig. 7. Backward motion field of frame 8 (B-frame) of the Flower Garden sequence: (a) without errors, (b) with errors, PER = 2%, estimated by: (c) MC-VM EC and (d) MVRI-CodM EC.

that justifies their remarkable property of being able to nonlinearly adapt their behavior with respect to local motion information and further establishes the observation that coding mode information is rather significant for EC purposes. In order to visually comprehend the performance of the motion field estimation methods, Fig. 7 shows the original, the erroneous, and the estimated motion fields produced by the MC-VM EC and MVRI-CodM EC methods. The erroneous or estimated part is included in a drawn rectangular with dashed lines. The observation of the estimated motion fields leads to the conclusion that the MVRI EC methods manage to retain the two characteristics of motion fields: motion uniformity in uniformly moving regions and motion discontinuity in irregularly moving regions, provided that the available neighboring motion information is adequate for estimating lost motion information.

Since real-time implementation capabilities are of great importance in order to allow decoding and concealment in real-time and in parallel, e.g., in digital TV signal transmission and reception, the processing time requirements of the presented EC methods are also examined. Execution time evaluation has been carried on a SGI Workstation R4400 at 200 MHz with 64-MB RAM. The results are tabulated in Table V. It is seen that the MVRI EC methods are rather fast, combining good performance and fast implementation, compared with other motion estimation EC methods under study. The MVE-BO EC and F-B BM EC methods present the slowest solutions due to the search they perform to re-estimate lost motion information.

TABLE V
EXECUTION TIMES IN SECONDS, REQUIRED FOR MOTION FIELD ESTIMATION BY THE EC METHODS UNDER STUDY, FOR ENTIRE SEQUENCE CONCEALMENT

EC Method	Flower	Mobile	Football
ZM EC	0.13	0.04	0.05
MC-AV EC	2.01	0.61	0.76
MC-VM EC	2.03	0.62	0.77
BMA EC	3.15	0.96	1.19
MVE-BO EC	108.88	30.89	39.79
F-B BM EC	806.77	492.89	572.82
BMFI EC	1.81	0.53	0.68
Comb BMFI	4.96	1.49	1.87
MVRI-2 – D EC	1.36	0.42	0.53
MVRI-2 – D-All EC	1.37	0.42	0.54
MVRI-BM EC	1.23	0.38	0.48
MVRI-RoC EC	1.47	0.45	0.58
MVRI-BMFI EC	1.94	0.60	0.76
MVRI-CodM EC	2.20	0.70	0.86

Finally, performance comparison among the different presented motion vector rational interpolation EC schemes follows aiming at clarifying which may actually be used under certain conditions. By observing all tables with PSNR, MFE, and execution time values and having visually compared many concealed frames by each one of the presented methods, we are led to the following remarks.

- The MVRI method that further exploits coding mode information achieves the best results with respect to PSNR and MFE values with only a small increase in the required computational time which still is low compared to the one required by state-of-the-art concealment methods.
- The second best proves to be the one interpolating in the direction of minimum change along with the one further using bilinear interpolation aspects, the latter being only slightly slower than the former.
- The MVRI method that also uses coding mode information leads to enhanced visual quality of the concealed frames.
- The above performances are almost similarly monitored for all test sequences considered.

Based on the above remarks, one could concluded that the best option among the MVRI methods to be used is the one exploiting coding mode information. However, when time constraints are rather demanding and since the performance of the other MVRI methods is not far behind, faster MVRI methods could be used.

V. CONCLUSIONS

Motion field estimation by motion vector rational interpolation has been investigated for EC purposes. A number of such interpolation schemes have been introduced. Motion vector

rational interpolation achieves to capture neighboring motion smoothness or irregularities and adapt its behavior with respect to the available information. It is proven that all MVRI schemes perform satisfactorily and are remarkably fast compared with other motion field estimation EC methods under study. The MVRI EC scheme that has the best interpolation performance additionally uses available adjacent coding mode information. The presented methods are able to deal with cases of low to medium PER values.

Another possible application of motion vector rational interpolation, apart from EC, could be the smoothing of motion fields, evaluated, e.g., by block matching approaches which are known to lead to many estimation errors, and their improved conversion from coarser to finer ones.

REFERENCES

[1] Y. Wang and Q.-F. Zhu, "Error control and concealment for video communication: A review," *Proc. IEEE*, vol. 86, pp. 974–997, May 1998.

[2] P. Salama, N. B. Shroff, and E. J. Delp, "Error concealment in encoded video streams," in *Signal Recovery Techniques for Image and Video Compression and Transmission*. Norwell, MA: Kluwer, 1998, pp. 199–233.

[3] X. Lee, Y. Zhang, and A. Leon-Garcia, "Information loss recovery for block-based image coding techniques – A fuzzy logic approach," *IEEE Trans. Image Processing*, vol. 4, pp. 259–273, Mar. 1995.

[4] H. Sun and W. Kwok, "Concealment of damaged block transform coded images using projections onto convex sets," *IEEE Trans. Image Processing*, vol. 4, pp. 470–477, Apr. 1995.

[5] W.-M. Lam and A. R. Reibman, "An error concealment algorithm for images subject to channel errors," *IEEE Trans. Image Processing*, vol. 4, pp. 533–542, May 1995.

[6] J. W. Park, J. W. Kim, and S. Lee, "DCT coefficients recovery-based error concealment technique and its application to the MPEG-2 bit stream error," *IEEE Trans. Circuits Syst. Video Technol.*, vol. 7, pp. 845–854, Dec. 1997.

[7] H. Sun, J. W. Zdepski, W. Kwok, and D. Raychaudhuri, "Error concealment algorithms for robust decoding of MPEG compressed video," *Signal Processing: Image Commun.*, vol. 10, no. 4, pp. 249–268, 1997.

[8] G.-S. Yu, M. M.-K. Liu, and M. W. Marcellin, "POCS-based error concealment for packet video using multiframe overlap information," *IEEE Trans. Circuits Syst. Video Technol.*, vol. 8, pp. 422–434, Aug. 1998.

[9] Z. Wang, Y. Yu, and D. Zhang, "Best neighborhood matching: An information loss restoration technique for block-based image coding systems," *IEEE Trans. Image Processing*, vol. 7, pp. 1056–1061, July 1998.

[10] S. Tsekeridou and I. Pitas, "MPEG-2 error concealment based on block matching principles," *IEEE Trans. Circuits Syst. Video Technol.*, vol. 10, pp. 646–658, June 2000.

[11] J. Zhang, J. F. Arnold, and M. R. Frater, "A cell-loss concealment technique for MPEG-2 coded video," *IEEE Trans. Circuits Syst. Video Technol.*, vol. 10, pp. 659–665, June 2000.

[12] M. Al-Mualla, N. Canagarajah, and D. R. Bull, "Temporal error concealment using motion field interpolation," *Electron. Lett.*, vol. 35, no. 3, pp. 215–217, Feb. 1999.

[13] W.-M. Lam, A. R. Reibman, and B. Liu, "Recovery of lost or erroneously received motion vectors," in *Proc. 1993 Int. Conf. Acoustics, Speech and Signal Processing*, vol. V, Apr. 1993, pp. 417–420.

[14] L. Khriji, F. A. Cheikh, and M. Gabbouj, "High-resolution digital resampling using vector rational filters," *SPIE Opt. Eng.*, vol. 38, no. 5, pp. 893–901, May 1999.

[15] F. A. Cheikh, L. Khriji, M. Gabbouj, and G. Ramponi, "Color image interpolation using vector rational filters," in *Proc. SPIE/EI Conf., Nonlinear Image Processing IX*, vol. 3304, San Jose, CA, Jan. 1998.

[16] L. Khriji, F. A. Cheikh, and M. Gabbouj, "Multistage vector rational interpolation for color images," in *Proc. 2nd IMACS-IEEE Int. Multiconf. Computational Engineering in System Application (CESA'98)*, Hammamet, Tunisia, Apr. 1998.

[17] I.-W. Tsai and C.-L. Huang, "Hybrid cell loss concealment methods for MPEG-II-based packet video," *Signal Processing: Image Commun.*, vol. 9, no. 2, pp. 99–124, 1997.

[18] S. Tsekeridou, F. A. Cheikh, M. Gabbouj, and I. Pitas, "Motion field estimation by vector rational interpolation for error concealment purposes," in *Proc. 1999 IEEE Int. Conf. Acoustics, Speech and Signal Processing*, Phoenix, AZ, Mar. 1999.

[19] F. A. Cheikh, L. Khriji, and M. Gabbouj, "Unsharp masking-based approach for color image processing," in *Proc. IX European Signal Processing Conf. (EUSIPCO'98)*, vol. II, Rhodes, Greece, Sept. 1998, pp. 1033–1036.

[20] G. Sapiro and D. L. Ringach, "Anisotropic diffusion of multivalued images with applications to color filtering," *IEEE Trans. Image Processing*, vol. 5, pp. 1582–1586, Nov. 1996.

[21] J. Scharcanski and A. N. Venetsanopoulos, "Edge detection of color images using directional operators," *IEEE Trans. Circuits Syst. Video Technol.*, vol. 7, pp. 397–401, Apr. 1997.

Sofia Tsekeridou (M'04) received the Dipl. Elect. Eng. in 1996 and the Ph.D. degree in informatics in 2001, both from Aristotle University of Thessaloniki, Thessaloniki, Greece.

During 1996–2001, she was involved in research activities under European and Greek funded R&D Projects, served as a Teaching Assistant and was also a Visiting Researcher at the Tampere University of Technology, Tampere, Finland. During 2001–2003, she was employed at the Development Programs Department, INTRACOM S.A., Greece, involved in R&D Projects dealing with next generation enhanced and interactive digital TV. Since 2003, she holds the position of Lecturer at the Electrical and Computer Engineering Department, Democritus University of Thrace, Xanthi, Greece. Her research interests lie in the areas of signal, image and video processing, computer vision, multimedia information systems, content- and semantic-based multimedia analysis and description. She co-authored over 40 publications, has contributed to the TV Anytime standardization body, and serves as a reviewer for many international conferences and scientific journals.

Dr. Tsekeridou is a member of the Technical Chamber of Greece.

Faouzi Alaya Cheikh received the B.S. degree in electrical engineering in 1992 from Ecole Nationale d'Ingenieurs de Tunis, Tunis, Tunisia, and the M.S. and the Ph.D. degrees in electrical engineering from Tampere University of Technology, Tampere, Finland in 1996 and 2004, respectively.

He is currently a Senior Researcher at the Institute of Signal Processing, Tampere University of Technology, Tampere, Finland. From 1994 to 1996, he was a Research Assistant at the Institute of Signal Processing, and since 1997, has been a Researcher with the same institute. His research interests include nonlinear signal and image processing and analysis, pattern recognition and content-based analysis and retrieval. He has been an active member in many Finnish and European research projects among them Nobless esprit, COST 211 quat, and MUVI. He co-authored over 30 publications.

Dr. Cheikh served as Associate Editor of the *EURASIP Journal on Applied Signal Processing* for the Special Issue on Image Analysis for Multimedia Interactive Services. He serves as a reviewer for several conferences and journals.

Moncef Gabbouj (SM'95) received the B.S. degree in electrical engineering from Oklahoma State University, Stillwater, in 1985, and the M.S. and Ph.D. degrees in electrical engineering from Purdue University, West Lafayette, IN, in 1986 and 1989, respectively.

He is currently a Professor and Head of the Institute of Signal Processing of Tampere University of Technology, Tampere, Finland. His research interests include nonlinear signal and image processing and analysis, content-based analysis and retrieval and video coding. He is co-author of over 250 publications.

Dr. Gabbouj served as Associate Editor of the IEEE TRANSACTIONS ON IMAGE PROCESSING. He is the past chairman of the IEEE Finland Section and the IEEE Circuits and Systems (CAS) Society, TC DSP, and the IEEE Signal Processing/CAS Finland Chapter. He was co-recipient of the Myril B. Reed Best Paper Award from the 32nd Midwest Symposium on Circuits and Systems and co-recipient of the NORSIG 94 Best Paper Award from the 1994 Nordic Signal Processing Symposium.

Ioannis Pitas (SM'94) received the Dipl. Elect. Eng. in 1980 and the Ph.D. degree in electrical engineering in 1985, both from the University of Thessaloniki, Thessaloniki, Greece.

Since 1994, he has been a Professor at the Department of Informatics, University of Thessaloniki, Greece. His current interests are in the areas of digital image processing, multimedia signal processing, multidimensional signal processing and computer vision. He has published over 450 papers, contributed in 17 books and authored, co-authored, edited, co-edited 7 books in his area of interest. HE is the co-author of the books *Nonlinear Digital Filters: Principles and Applications* (Norwell, MA: Kluwer, 1990) and *3D Image Processing Algorithms* (New York: Wiley, 2000), is the author of the books *Digital Image Processing Algorithms* (Englewood Cliffs, NJ: Prentice Hall, 1993), *Digital Image Processing Algorithms and Applications* (New York: Wiley, 2000), *Digital Image Processing* (in Greek, 1999), and is the editor of the book *Parallel Algorithms and Architectures for Digital Image Processing, Computer Vision and Neural Networks* (New York: Wiley, 1993) and co-editor of the book *Nonlinear Model-Based Image/Video Processing and Analysis* (New York: Wiley, 2000). He is/was principal investigator/researcher in more than 40 competitive R&D projects and in 11 educational projects, all mostly funded by the European Union.

Dr. Pitas is/was Associate Editor of the IEEE TRANSACTIONS ON CIRCUITS AND SYSTEMS, IEEE TRANSACTIONS ON NEURAL NETWORKS, IEEE TRANSACTIONS ON IMAGE PROCESSING, IEICE, *Circuits Systems and Signal Processing*, and was co-editor of *Multidimensional Systems and Signal Processing*. He was Chair of the 1995 IEEE Workshop on Nonlinear Signal and Image Processing (NSIP95), Technical Chair of the 1998 European Signal Processing Conference, and General Chair of IEEE ICIP2001. He was co-chair of the 2003 International workshop on Rich media content production. He was technical co-chair of the 2003 Greek Informatics conference (EPY).